Simulation of alpha particle current drive and heating in spherical tokamaks

R. Farengo[1], M. Zarco[1], H. E. Ferrari[1,2]
[1]Centro Atómico Bariloche and Instituto Balseiro, Argentina.
[2] Consejo Nacional de Investigaciones Científicas y Técnicas (CONICET), Argentina

Abstract

A Monte Carlo code is employed to study plasma heating and current drive by alpha particles in small aspect ratio tokamaks. Equilibria with different aspect ratios and density and temperature profiles are considered. Good alpha particle confinement and high deposited power fraction is observed. The alpha particle current is relatively small and shows a very weak aspect ratio dependence.

1 Introduction

The behavior of alpha particles is of critical importance in fusion reactors. They provide most of the heating, can contribute to the plasma current and can trigger instabilities. In addition, escaping alpha particles can damage the first wall and alpha particle pressure can significantly contribute to the total pressure, thus affecting the density and temperature profiles.

Small aspect ratio tokamaks ("spherical tokamaks", ST) are considered interesting candidates for the development of fusion reactors or neutron sources for material studies and a number of conceptual designs covering both options have been presented in the last few years [1] [2]. In this paper we present a detailed study of alpha particle heating and current drive in STs. We employed a Monte Carlo code [3] to calculate the power deposited in the plasma and the current generated by the alpha particles produced in D-T fusion reactions in small aspect ratio tokamaks. The code follows the exact trajectories (no gyro-averaging) and includes particle drag and pitch angle scattering. Equilibria with different aspect ratios and density and temperature profiles were analyzed.

The current driven by fusion produced alpha particles can contribute to the total current in tokamak reactors. Tani and Azumi [4] recently studied current generation by alpha particles in ITER and a relatively small aspect ratio ($A \approx 1.95$) tokamak. In their code, the guiding-center equations are integrated numerically and collisional effects included with a Trubnikov type collision operator. Using the guiding-center equations is justified in large aspect ratio, high field, tokamaks but not in STs. In a ST reactor with the parameters given in Ref. [1], the Larmor radius (ρ_α) is of the same order as the banana width and $\rho_\alpha/a \sim 0.05$, where a is the minor radius.

In all the equilibria considered good alpha particle confinement was observed, with very small prompt losses. The deposited power fractions were high and depended on the shape of the equilibrium. The spatial distribution of lost particles was quite uniform, with more particles lost on the low field side but without localized "hot" spots. The current produced by the alpha particles was around 3-4% of the total current, and showed a very weak dependence on the aspect ratio.

This paper is organized as follows. In section 2 we describe the equilibrium and basic plasma parameters and in section 3 present a brief account of the numerical methods employed. Section 4 contains the results on plasma heating by alpha particles while section 5 has the results on current drive. Finally, in section 6 we summarize our findings.

2 Equilibrium

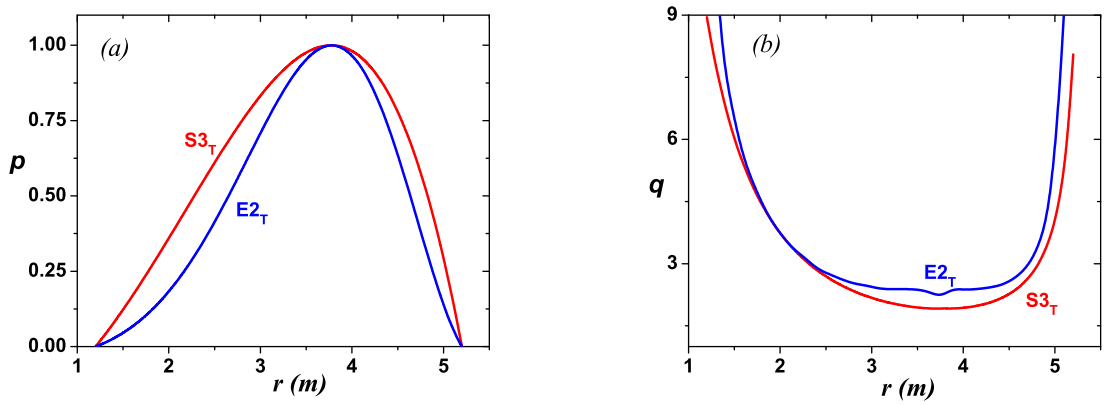

Figure 1: Pressure (a) and safety factor profiles (b) of equilibria S3$_T$ and E2$_T$.

Two types of plasma equilibria were employed. The first one is a simple analytical solution of the Grad-Shafranov (G-S) equation (Solov'ev equilibrium) [5] which has already been used to model STs. The second one was obtained by numerically solving the G-S equation with a pressure and poloidal current of the form:

$$p(\psi) = G_0 \left[\frac{\psi}{\psi_0} - \frac{C}{2} \left(\frac{\psi}{\psi_0} \right)^2 \right], \quad I_p(\psi) = I_0 + I_1 \left(\frac{\psi}{\psi_0} \right) \tag{1}$$

where G_0 is a constant, ψ_0 is the maximum poloidal magnetic flux and the constant C determines the shape of the current profile (hollow for $C > 0$ and peaked for $C < 0$). The main plasma

	A	$R_0(m)$	$a(m)$	κ	q_0	q_{95}	$I(MA)$	$B_e(T)$	$n_e(10^{20}m^{-3})$	$E(MJ)$
$S1_T$	1.4	2.8	2.0	3.55	1.93	8.81	29.0	2.14	1.86	514, 0
$S2_T$	1.5	3.0	2.0	3.55	1.91	7.11	29.0	2.14	1.86	559, 9
$S3_T$	1.6	3.2	2.0	3.55	1.92	6.24	29.0	2.14	1.86	605, 4
$S4_T$	1.8	3.6	2.0	3.55	1.85	4.77	29.0	2.14	1.86	695, 3
$S5_T$	2.0	4.0	2.0	3.55	1.80	3.86	29.0	2.14	1.86	784, 1
$S1_n$	1.4	2.8	2.0	3.55	1.94	8.79	29.0	2.14	1.59	514, 0
$S2_n$	1.5	3.0	2.0	3.55	1.89	7.09	29.0	2.14	1.59	559, 3
$S3_n$	1.6	3.2	2.0	3.55	1.91	7.6	29.0	2.14	1.59	605, 4
$S4_n$	1.7	3.4	2.0	3.55	1.87	5.29	29.0	2.14	1.59	650, 5
$S5_n$	1.8	3.6	2.0	3.55	1.86	5.12	29.0	2.14	1.59	695, 3
$S6_n$	2.0	4.0	2.0	3.55	1.79	3.86	29.0	2.14	1.59	784, 0
$S7_n$	2.2	4.4	2.0	3.55	1.71	3.35	29.0	2.14	1.59	871, 9

Table 1: Parameters of S-type equilibria.

parameters were taken to be similar to those employed in the ARIES-ST study [1]. Starting with the aspect ratio employed in Ref. [1] ($A = 1.6$) we varied A over a wide range by changing the major radius (R_0) while keeping the minor radius constant at $a = 2\ m$. The plasma current (I), toroidal field at R_0 (B_e), peak electron density (n_e) and elongation at the separatrix (κ) were kept approximately constant. Table 1 lists the parameters of the Solov'ev type equilibria (S equilibria) considered and Table 2 those of the numerical solutions of the G-S equation obtained using eq. (1) (E equilibria). The other parameters shown in Tables 1 and 2 are the safety factor on axis (q_0) and at the 95% flux surface (q_{95}) and the plasma energy content (E). Since

the G-S equation only gives the pressure profile there is some freedom in choosing the density and temperatures profiles. We have considered two, extreme, cases; uniform density with non uniform temperature, and uniform temperature with non uniform densities. This is indicated with a subscript n or T (i.e. $S1_n$ or $S1_T$) for the uniform density and uniform temperature equilibria respectively. S-type equilibria with uniform temperature have $T_e = T_i = 16.5$ keV while those with uniform density have a peak temperature of 19.5 keV. For the E-type equilibria we used 16.5 keV for both cases. Note that this choice affects the plasma parameters and collision rates and also the distribution of the alpha particle source (see below). Fig. 1 shows the pressure and safety factor profiles of equilibria S3 and E2.

	A	$R_0(m)$	$a(m)$	κ	q_0	q_{95}	$I(MA)$	$B_e(T)$	$n_e(10^{20}m^{-3})$	$E(MJ)$
$E1_T$	1.4	2.8	2.0	3.48	2.13	16.1	26.8	2.14	1.59	400.2
$E2_T$	1.6	3.2	2.0	3.47	2.19	8.47	27.8	2.14	1.59	550.3
$E3_T$	1.8	3.6	2.0	3.47	1.80	5.7	27.8	2.14	1.59	619.9
$E4_T$	2.0	4.0	2.0	3.47	2.54	6.0	30.0	2.14	1.62	799.3
$E1_n$	1.4	2.8	2.0	3.47	2.17	8.9	29.6	2.14	1.60	405.9
$E2_n$	1.6	3.2	2.0	3.47	2.04	7.5	28.6	2.14	1.60	457.2
$E3_n$	1.8	3.6	2.0	3.47	1.89	6.3	28.6	2.14	1.59	507.4
$E4_n$	2.0	4.0	2.0	3.47	1.75	5.3	27.5	2.14	1.60	560.3

Table 2: Parameters of E-type equilibria

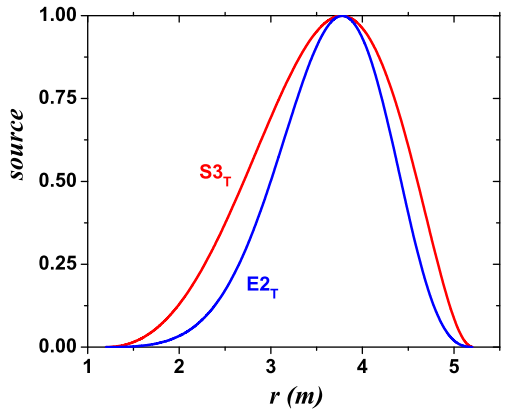

Figure 2: Alpha particle source of equilibria $S3_T$ and $E2_T$.

Alpha particles are produced at a rate that depends on the local density and temperature:

$$S_\alpha = n_D\, n_T\, \langle \sigma v \rangle \tag{2}$$

where S_α is the number of alpha particles produced per unit volume per second, n_D and n_T are the deuterium and tritium densities ($n_D = n_T$ in all cases considered) and $\langle \sigma v \rangle$ is the fusion reaction rate, which depends on the temperature. Fig. 2 shows the spatial dependence of the alpha particle source for equilibria $S3_T$ and $E2_T$.

3 Numerical methods

The equilibrium and particle codes employed in this study have already been used to study the interaction of neutral beams and fusion particles with Field Reversed Configuration plasmas [6], [3]. The numerical solutions of the Grad-Shafranov equation were obtained with a semi-implicit

alternating-direction-implicit solver [7]. Since the current produced by the alpha particles is a small fraction of the total plasma current, its contribution was not included in the equilibrium, which remained fixed. In all the calculations we assumed that the plasma was in a stationary equilibrium, where all parameters remained constant. This means that we assumed that the energy deposited by the alpha particles simply compensated the losses, which were not calculated. A full transport code would be needed to calculate the effect of all the heating and losses on the plasma profiles. This is beyond the scope of this paper.

The Monte Carlo particle code calculates the trajectories of the ions solving the following stochastic equation:

$$\frac{d\mathbf{u}}{dt} = \frac{q}{m}\left(\mathbf{u}\times\mathbf{B}\right) - \nu\mathbf{u} + \underline{\mathrm{D}}\,\mathbf{.}\,\mathbf{u} \tag{3}$$

where q and m are the particle charge and mass, $\mathbf{u}$ its velocity and $\mathbf{B}$ the equilibrium magnetic field. The last two terms in equation (3) contain the effect of collisions; ν is the friction coefficient and $\underline{\mathrm{D}}$ the diffusion tensor of a Brownian particle in velocity space [8].

The particles are initially distributed in space with a density proportional to the local fusion reaction rate. In velocity space the initial distribution is isotropic. The initial velocity is defined by three numbers: the absolute value and the polar and azimuthal angles. The absolute value is determined by fixing the energy (3.5 MeV) and the polar and azimuthal angles are chosen by generating two random numbers. The method employed to obtain stationary values for the desired quantities (current density, deposited power, etc.) from the information on individual particles is similar to the one employed in Ref. [4]. Most of the results presented below were obtained by following approximately 2×10^5 particles for each set of equilibrium parameters.

4 Heating

Tables 3 and 4 show the results obtained for the different equilibria considered. Good alpha particle confinement was observed in all cases and no "hot" spots (regions of localized particle losses) have been found. The deposited power fraction ranges from approximately 86% for

	$P_g\ (MW)$	$P_d\ (MW)$	$P_e\ (MW)$	$P_i\ (MW)$
$S1_T$	297.8	282.9	203.2	79.7
$S2_T$	325.0	310.8	223.2	87.6
$S3_T$	352.1	337.6	242.4	95.2
$S4_T$	405.7	391.2	280.8	110.4
$S5_T$	458.7	444.3	318.9	125.5
$S1_n$	335.8	331.8	247.8	84.0
$S2_n$	366.7	362.4	270.6	91.7
$S3_n$	397.4	392.7	293.3	99.3
$S4_n$	427.9	422.9	315.8	107.1
$S5_n$	458.2	452.8	337.8	114.9
$S6_n$	518.4	512.2	382.4	129.8
$S7_n$	577.8	571.	426.1	144.9

Table 3: Total generated power, total deposited power, power deposited in electrons and power deposited in ions for S-type equilibria.

E-type equilibria with uniform temperature ($E1_T - E4_T$) to 97-99% for the equilibria with uniform density (both types). It is reasonable that equilibria with uniform density show better alpha particle confinement because higher density and lower temperature result in a higher collision rate. The power deposited in the ions is always significantly smaller than the power deposited in the electrons. For S-type equilibria the ratio P_i/P_e is approximately 39% for uniform temperature and 34% for uniform density while for E-type equilibria it is approximately 37%

	$P_g\ (MW)$	$P_d\ (MW)$	$P_e\ (MW)$	$P_i\ (MW)$
$E1_T$	$179,45$	$156,40$	$114,07$	$42,32$
$E2_T$	$257,17$	$221,21$	$162,13$	$59,08$
$E3_T$	$291,22$	$255,17$	$186,04$	$69,12$
$E4_T$	$397,22$	$355,17$	$258,16$	$97,00$
$E1_n$	$197,3$	$192,21$	$154,02$	$38,19$
$E2_n$	$220,6$	$218,17$	$175,02$	$43,15$
$E3_n$	$242,79$	$225,66$	$178,12$	$47,53$
$E4_n$	$267,72$	$264,74$	$211,98$	$52,75$

Table 4: Total generated power, total deposited power, power deposited in electrons and power deposited in ions for E-type equilibria.

for uniform temperature and 25% for uniform density. It is clear that equilibria with uniform temperature will have a larger plasma volume with high temperature thus increasing the power deposited in the ions. Increasing the peak temperature for S-type equilibria with uniform density increases the ratio P_i/P_e up to 41% for $T_e = 24keV$. We note that approximate equipartition was reported in [2] for $T_e = 24keV$.

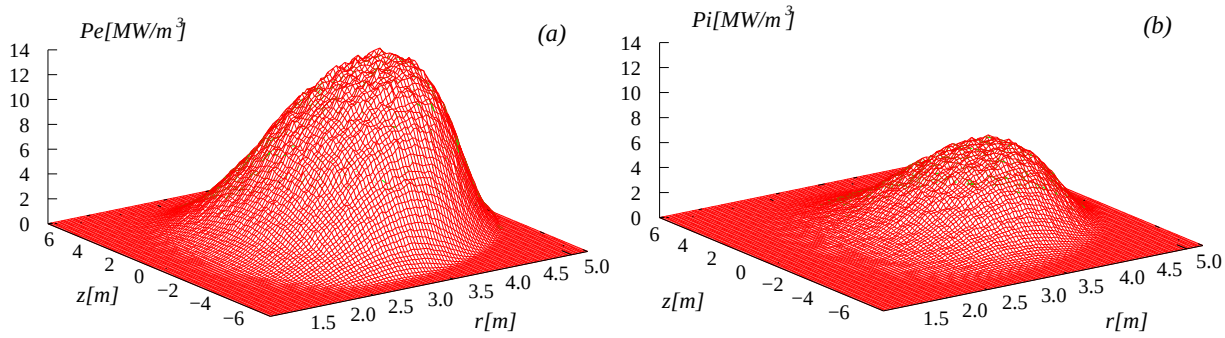

Figure 3: Spatial distribution of the power deposited in electrons (a) and ions (b) for equilibrium S3$_T$

Figure 3 shows the spatial distribution of the power deposited in electrons and ions for equilibrium $S3_T$ while Fig. 4 presents the same information for equilibrium $E2_T$. It is clear that the profiles corresponding to equilibrium $S3_T$ are broader than those of equilibrium $E2_T$. This is seen more clearly in Fig. 5 which shows the radial distribution of the heating profile at the midplane ($z = 0$) for the same equilibria. We note, comparing Fig. 5 with Fig. 2 that the heating profiles are broader than the source profiles.

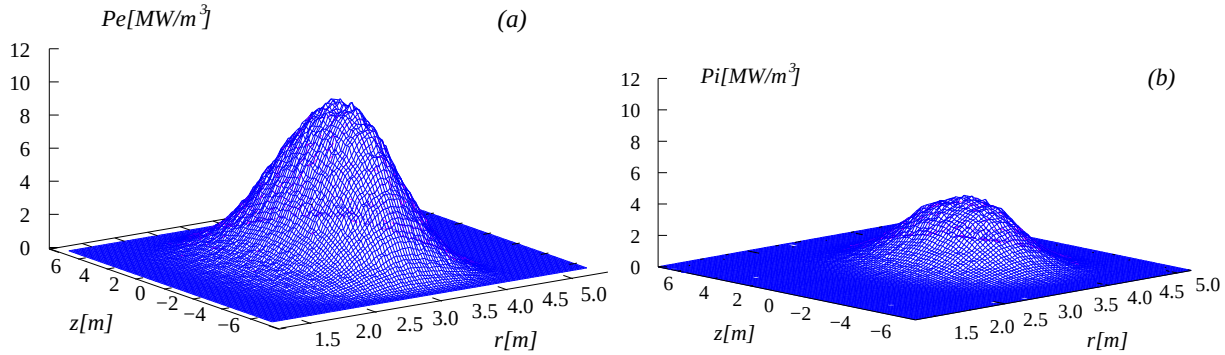

Figure 4: Spatial distribution of the power deposited in electrons (a) and ions (b)for equilibrium E2$_T$

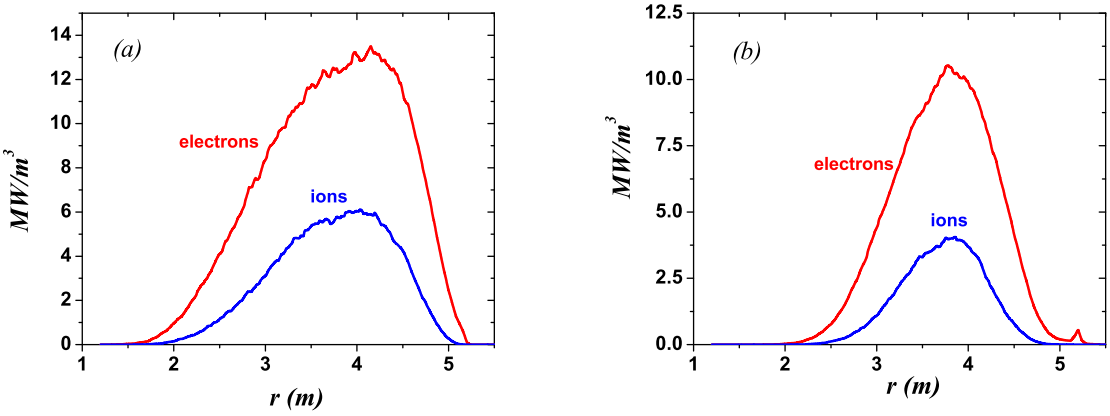

Figure 5: Radial distribution of the heating profiles at the midplane ($z = 0$) for equilibria $S3_T$ (a) and $E2_T$ (b)

5 Current

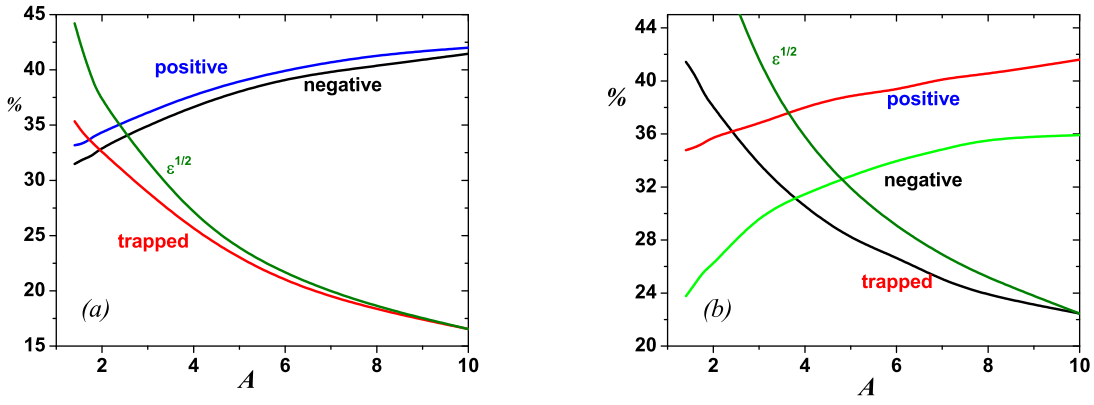

Figure 6: Fraction of 20 keV trapped, positive and negative particles for equilibria with $B_{pol} << B_{tor}$ (a) and fraction of 3.5 MeV trapped, positive and negative particles for equilibria with $B_{pol} \sim B_{tor}$ (b)

Trapped and passing alpha particles contribute to the total current. Passing particles can be further divided into *positive*, those that rotate around the tokamak in the same sense as the plasma current, and *negative*, those that rotate in the opposite sense. The fraction of particles of each type is critical to determine the resulting current. Chu [9] showed the existence of an asymmetry with respect to the parallel velocity in the trapping boundary that results in diferent fractions of positive and negative passing particles. This asymmetry depends on the ratio between the width of the orbit and the radius of the flux surface and therefore increases with the particle energy and with the inverse aspect ratio ($\varepsilon = A^{-1}$).

For thermal ions in conventional tokamaks, with large aspect ratio ($\varepsilon << 1$) and low poloidal field ($B_{pol}/B_{tor} << 1$), the trapped particle fraction scales approximately as $\sqrt{\varepsilon}$ and the difference between the fractions of positive and negative passing particles is relatively small. For high energy particles in STs this is not the case. The trapped particle fraction is larger and presents a relatively weaker dependence on the aspect ratio while the difference between positive and negative passing particles is much larger. To clarify this issue we employed the numerical code described above (without collisions) to calculate the fractions of trapped, positive and negative

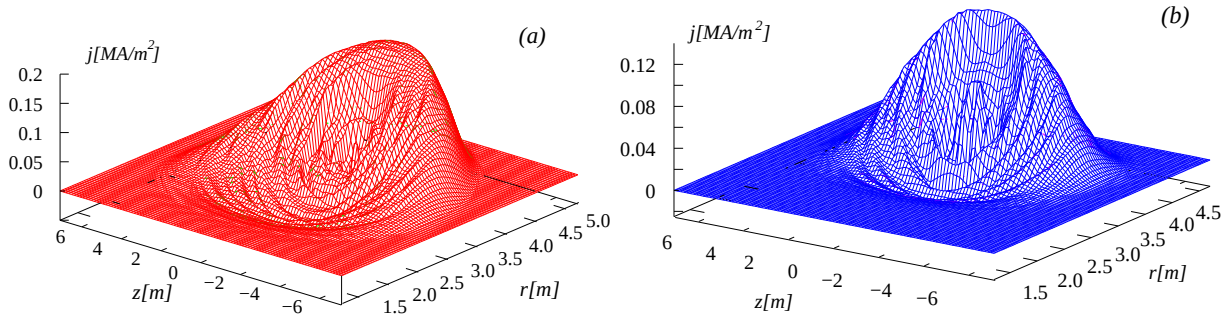

Figure 7: Spatial distribution of the current density for equilibria $S3_T(a)$ and $E2_T$ (b)

passing particles for different aspect ratios, energies and values of B_{pol}/B_{tor}. Two families of Solov'ev type equilibria were considered. The first one is the same shown in Table 1, continued to larger aspect ratios, and has $B_{pol}/B_{tor} \sim 0.5$. The second family has a larger toroidal field and a smaller plasma current resulting in $B_{pol}/B_{tor} \sim 0.1$. A large number of particles with the same energy, random velocity directions, and distributed according to the fusion reaction rate were followed to determine if they were positive, negative or trapped. The results are shown in Fig. 6.

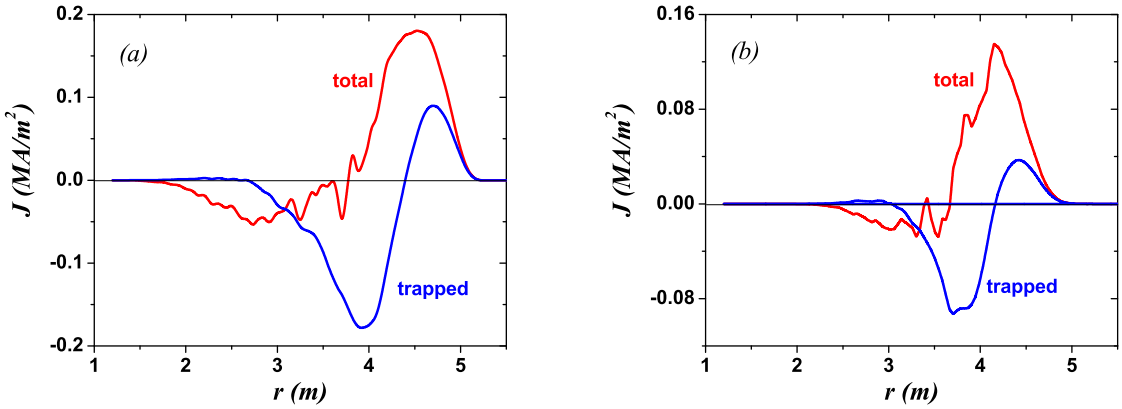

Figure 8: Current density profile for equilibria $S3_T(a)$ and $E2_T$ (b)

Tables 5 and 6 shows the current produced by trapped alpha particles (I_b) and the total alpha particle current (I_{tot}) for the equilibria indicated in Tables 1 and 2. It is seen that in spite of the large differences between the fractions of positive and negative particles at low A, the current is relatively small (less than 3% of the total plasma current). There are two reasons for this low current:

1. The relatively high density of the equilibria considered that results in a large collision frequency (small mean free path).

2. The negative contribution of the alpha particle current at low A, where the unbalance between positive and negative passing particles is larger.

We also note a very weak aspect ratio dependence. As the aspect ratio decreases the negative (in most cases) trapped particle current increases, compensating the increase in the unbalance between positive and negative passing particles. We note that the shape of the equilibrium afects the results, with the trapped particle current being positive for E-type equilibria with uniform density.

	$I_\alpha(MA)$	$I_{tot}(MA)$
$S1_T$	-0.178	1.008
$S2_T$	-0.175	0.947
$S3_T$	-0.147	1.035
$S4_T$	-0.122	1.048
$S5_T$	-0.118	0.995
$S1_n$	-0.401	1.106
$S2_n$	-0.294	1.169
$S3_n$	-0.275	1.056
$S4_n$	-0.047	1.188
$S5_n$	-0.097	1.199
$S6_n$	-0.038	1.116
$S7_n$	0.027	1.196

Table 5: Current produced by trapped alpha particles (I_b) and the total alpha particle current (I_{tot}) for the equilibria indicated in Tables 1

	$I_\alpha(MA)$	$I_{tot}(MA)$
$E1_T$	-0.007	1.11
$E2_T$	-0.007	0.77
$E3_T$	-0.009	1.29
$E4_T$	-1.17	0.93
$E1_n$	0.029	0.65
$E2_n$	0.031	0.62
$E3_n$	0.043	0.57
$E4_n$	0.046	0.58

Table 6: Current produced by trapped alpha particles (I_b) and the total alpha particle current (I_{tot}) for the equilibria indicated in Tables 1 and 2

6 Summary

We studied alpha particle heating and current drive in small aspect ratio tokamaks. Two types of equilibria, which remained fixed, were employed and the aspect ratio was varied over a wide range, while keeping the other parameters approximately constant. A Monte Carlo code that follows the exact alpha particle trajectories and includes pitch angle scattering and diffusion was employed.

Good alpha particle confinement with very small prompt losses and high heating efficiency was observed. The power is deposited mostly in the electrons, even at relatively high temperatures ($T_e = 24\ keV$).

Trapped and passing particles contribute to the alpha particle current, which shows a very weak aspect ratio dependence. In most cases the positive current produced by the unbalance between positive and negative passing particles is partially compensated by the negative current produced by trapped particles. As expected, higher currents were obtained with higher temperature and lower density equilibria.

References

[1] F. Najmabadi and the Aries team, Fusion Eng. and Design, **65**, 143 (2003).

[2] G. M. Voss et al. Fusion Engineering and design **51-52**, 309 (2000).

[3] H. E. Ferrari, R. Farengo, Plasma Phys. Contrl. Fusion **49**, 713, (2007). H. E. Ferrari, R. Farengo,Nuclear Fusion, **48**, 035014, (2008).

[4] K. Tani, M. Azumi, Nucl. Fusion **48**, 085001 (2008).

[5] L. S. Solov'ev Sov. Phys. JETP **26**, 400 (1968).

[6] A. F. Lifschitz, R. Farengo, and N. R. Arista, Plasma Phys. Control. Fusion, **44**, 1979 (2002).

[7] R. L. Spencer and D. W. Hewett, Phys. Fluids, **25**, 1365 (1982)

[8] .S. Ichimaru, Basic Principles of Plasma Physics, p. 233, W. A Benjamin, Reading, Massachusetts 1971.

[9] T. K. Chu, Phys. Plasmas **3**, 3397 (1996).